Journal of Physics: Conference Series **599** (2015) 012042 doi:10.1088/1742-6596/599/1/012042

Investigation of prompt γ ray emission for online monitoring in ion therapy

D Steinschaden[1], S E Brunner[1], H Dichtl[2], H Fuchs[3,4,5], D Georg[3,4,5], A Hirtl[6], J Marton[1] and A Pichler[1]

[1] Stefan Meyer Institute for Subatomic Physics, Austrian Academy of Sciences, Austria
[2] University of Applied Sciences Upper Austria, Austria
[3] Christian Doppler Laboratory for Medical Radiation Research for Radiation Oncology, Medical University of Vieanna, Austria
[4] Department of Radiation Onkology, Medical University of Vienna / AKH Vienna, Austria
[5] Comprehensive Cancer Center, Medical University of Vienna /AKH Vienna, Austria
[6] Division of Nuclear Medicine, Department of Biomedical Imaging and Image-guided Therapy, Medical University of Vienna / AKH Vienna, Austria

E-mail: dominik.steinschaden@oeaw.ac.at

Abstract.

The aim of this study was to investigate the principle of using prompt γ ray emissions for the determination of the position of the Bragg peak in radiotherapy with carbon ions. Developing a system for online monitoring in ion therapy with the required accuracy is an important step for the utilization of modern accelerator facilities for medical purposes. The investigations were carried out by Monte Carlo studies in the framework of the simulation environment GATE. In the course of these investigations, production parameters of prompt γ rays, like the emission rate and energy distribution were determined as a function of the primary carbon ion energy and the penetration depth in a water target. A possible connection between these parameters and the position of the Bragg peak and the dose delivery was investigated. Within the energy spectrum an energy range was identified in which the production rate of the γ rays shows a significant drop right after the Bragg peak.

1. Introduction

The number of medical centres with focus on cancer treatment based on ion therapy increased during the last years [1]. Near Vienna the treatment facility MedAustron will start the treatment of patients in 2015 with proton and carbon ion beams [2]. In order to perform a therapy the patients are examined by established imaging methods and a treatment plan is calculated. Up to now, no direct and precise method for online monitoring of the distributed dose exists, which fulfils the required high accuracy combined with fast data collection and processing. A few promising techniques have been proposed and some are being investigated in pre-clinical research. So far only Positron-Emission-Tomography (PET) offers a technically feasible method for monitoring the dose distribution shortly after the dose delivery [3]. A possible alternative to PET monitoring is the detection of prompt γ radiation during radiotherapy. In contrast to the method of PET monitoring which is based on the β^+ decay, the prompt γ ray emission which is based on nuclear reactions happens on a time scale of less than 1 ns after the energy deposition.

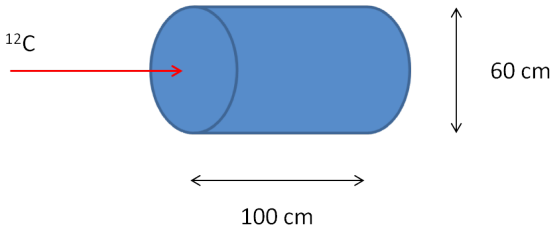

Figure 1. Simulation setup for investigations of the prompt γ ray production parameters. A carbon ion beam is aimed at a cylindrical water target along its longitudinal axis.

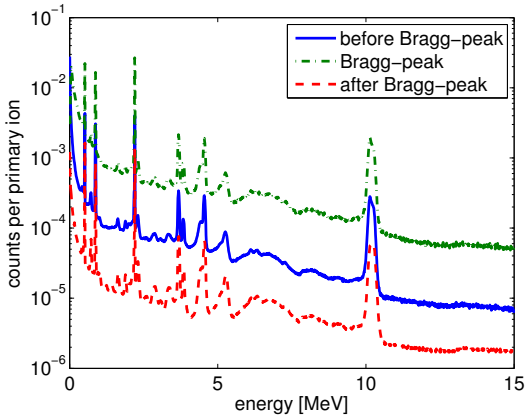

Figure 2. Spectra of γ rays produced by the irradiation of a water phantom with carbon ion at energies of 240 MeV/A. The solid line maps the energy spectrum before, the dashed dotted line at and the dashed line after the Bragg peak.

Therefore, prompt γ based monitoring does not suffer from physiological processes and high radiation background [4][5]. This approach was already experimentally demonstrated [6].

2. Material and Methods

The presented studies were realised within the simulation framework GATE (GEANT4 Application for Tomographic Emission) which is a modular and versatile toolkit for nuclear medicine [7], developed by the OpenGATE collaboration [8]. It is based on the simulation toolkit GEANT4 which contains modules to realise a complete range of functionalities and which can handle many different processes, particles and materials in an energy range from 250 eV up to a few TeV [9]. A verification of the simulated prompt γ spectra with experimental data has been performed with the results presented in reference [10]. Discrepancies of the simulated count rate up to the factor 2 has been observed in reference [11].

The simulation setup consisted of a cylindrical water target with a radius of 30 cm and a length of 100 cm which was assumed homogeneous. The phantom was irradiated with carbon ions along its longitudinal axis. The energy of the used ion beams varied from 120 MeV/A to 400 MeV/A corresponding to medical applications. The radial intensity distribution of the beam was Gaussian-shaped with an initial standard deviation of 3 mm and zero beam divergence (see Fig. 1).

In order to find a correlation between the Bragg peak, which was defined in this work as the position of the maximum dose deposit inside the irradiated target, ideal detectors were used to study the properties of prompt γ rays. The cylindrical target was divided into an inner section represented by a cylinder with a radius of 6 mm and a height of 100 cm centered along the longitudinal axis, which corresponds to 2 sigma of the used primary particle beam and an outer section which covered the rest of the water target. During the simulation, for each section the number of produced photons as a function of the penetration depth was accumulated in steps of 1 mm. Additionally, the number of produced photons was recorded up to 12 MeV in steps of 100 keV. Additional energy spectra of the produced γ rays were recorded for three subvolumes from the entrance face of the target until 5 mm prior to the Bragg peak, $\pm$ 5 mm around the Bragg peak and from 5 mm after the Bragg peak until the end of the target.

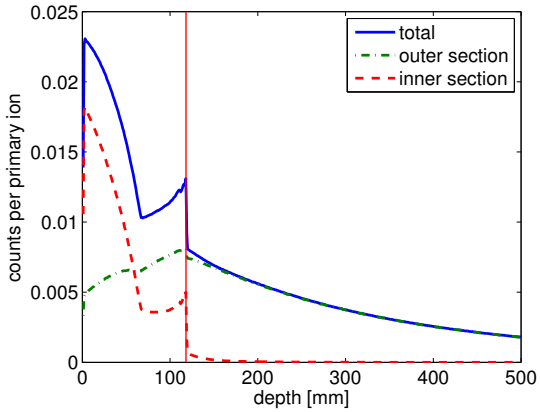

Figure 3. Production rate of prompt γ rays per primary carbon ion plotted for the different target regions as a function of the penetration depth. The red vertical line marks the position of the maximum dose deposit.

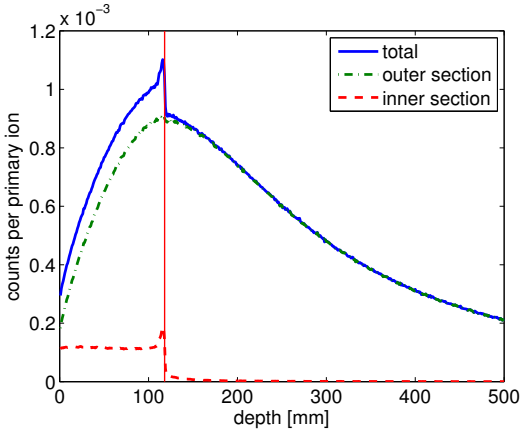

Figure 4. Photon production rates for photon energies of 2.2 ± 0.1 MeV plotted for different target regions as a function of the penetration depth. The position of the Bragg peak is marked by the red vertical line.

3. Results

Figure 2 shows the normalised energy spectra per cm for the 3 different target regions. Analysing the energy spectra did not result in finding a specific photon production process, which could be linked to the position of the Bragg peak. Apart from the count rate, the behaviour of the spectra remain the same for every penetration depth. A drop in the count rate could be identified after the Bragg peak.

An evaluation of the collected data with regard to the production rate for the different γ energies showed a significant difference. The total production rate is plotted in Figure 3 as a function of the penetration depth of the primary carbon ions with energies of 240 MeV/A.

Investigations showed that the high count rates in the area prior to the Bragg peak are mainly caused by photons with energies below 0.5 MeV. The rise in count rates at the Bragg peak and the drop afterwards is driven by photons with energies above 0.5 MeV. Figure 3 contains the production rate for photons separated into the inner and the outer section. While the production rate in the inner section drops almost immediately to zero after the Bragg peak, the drop in the count rate in the outer section is less significant. Consequently, the influence of this drop around the Bragg peak is less significant in the total photon production.

Similar results were observed for many of the prominent peaks of the energy spectra. As an example, in Figure 4 the production rates for 2.2 MeV γ rays are plotted as a function of depth for a primary energy of 240 MeV/A. These are mainly caused excited nuclei, which result from neutron capture of hydrogen and belong to the most prominent peak in the spectrum. Again, the production rate in the inner section shows a very significant drop after the Bragg peak, whereas the photon production of the outer section misses this effect. Due to the higher production rates in the outer section the significance of the drop is suppressed and thus, can not be used for the determination of the Bragg peak.

Although the effect is less drastic for other prominent peaks of the energy spectrum, the result remains comparable. Further analysis of the collected data showed that the significance of produced γ rays apart from the most prominent peaks rises. Also wider ranges of photon energies can be merged to increase both count rates and significance as Figure 5 shows for photon energies from 2.3 MeV to 6 MeV. In this energy range the production rate of γ rays inside the

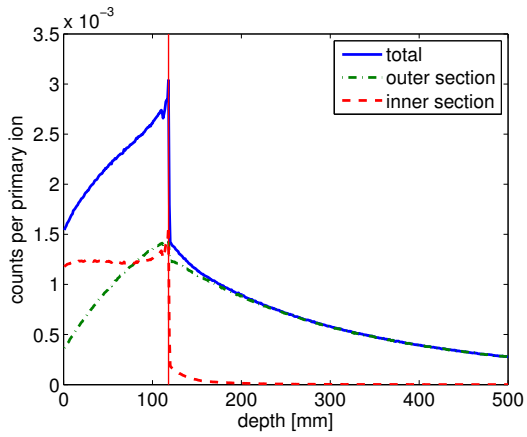

Figure 5. Production rates of γ rays with an energy from 2.3 to 6 MeV as a function of the penetration depth for the different target sections. The red vertical line marks the Bragg peak.

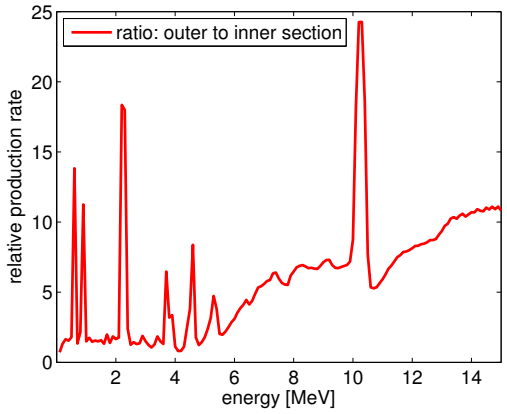

Figure 6. Relative γ ray production rate comparing the outer to the inner section of the target as a function of the γ ray energies. A lower value means less amount of outer photons, and therefore a more usable signal at the Bragg peak.

2 sigma range of the primary ion beam is even higher compared to the production in the outer section at the position of maximum dose deposition, which is marked by the red vertical line.

To get an overview of γ ray energies with a beneficial production rate, Figure 6 shows the relative photon production rate of the outer section to the inner section for 240 MeV/A primary carbon ions as a function of the photon energy. In confirmation of the studies above, the prominent peaks of the energy spectra show a significantly higher ratio of outer to inner γ rays. Also the values of the ratio for photons produced with energies higher then 6 MeV are above the average of the energy range of 2.3 - 6 MeV photons.

4. Discussion

Although the energy spectra do not reveal a significant photon energy which can be linked to the Bragg peak, the data show a strong correlation of the photon production rate and the position of maximum dose deposit visible by a drop in the production function. This signal is very sharp for photons produced in the inner section of the target most likely due to collisions of primary particles. γ rays produced outside of the 2 sigma range of the primary beam lower the visibility of the drop at the Bragg peak since they are produced with a high probability by secondary or scattered particles. An increase of the signal could be achieved by focusing on a energy range of produced γ rays with a beneficial ratio of outer to inner production rate. Such an energy range was found for γ rays between 2.3 MeV and 6 MeV which seems the most utilisable energy range for determining the Bragg peak.

5. Conclusion

The presented data provide a possibility to relate the production rate of prompt γ rays to the position of the Bragg peak, i.e., the point of the maximum dose deposition. Further investigations are necessary to develop a detector system to determine and monitor the spatial distribution of the deposited energy. Although optimization needs to be done, for typical medical beam rates online monitoring, based on prompt γ rays, seems to be feasible.

Acknowledgments
The main part of the work was performed on the computer cluster of the MOCCAMED group which enabled simulations with sufficient statistics in reasonable time. The project was financially supported by the Federal Ministry of Economy, Family and Youth and the National Foundation for Research, Technology and Development.

References
[1] Giap F N, Giap H B, Mazal A, Jermann M, Giap B, Levy R P and Blomquist E 2013 *Translational Cancer Research* **1**
[2] Medaustron `http://www.medaustron.at/` [Online; accessed 28-July-2014]
[3] Parodi K 2012 *Nuclear Medicine Review* **15** C37
[4] Testa E, Bajard M, Chevallier M, Dauvergne D, Foulher F L, Freud N, Letang J M, Poizat J C, Ray C and Testa M 2008 *Applied Physics Letters* **93** 093506
[5] Schardt D, Elsässer T and Schulz-Ertner D 2010 *Rev. Mod. Phys.* **82** 383–425
[6] Testa E, Bajard M, Chevallier M, Dauvergne D, Foulher F L, Freud N, Ltang J, Poizat J, Ray C and Testa M 2009 *Nuclear Instruments and Methods in Physics Research Section B: Beam Interactions with Materials and Atoms* **267** 993–6
[7] Jan S *et al.* 2011 *Physics in Medicine and Biology* **56** 881–901
[8] 2013 www.opengatecollaboration.org
[9] Agostinelli S *et al.* 2003 *Nuclear Instruments and Methods in Physics Research Section A: Accelerators, Spectrometers, Detectors and Associated Equipment* **506** 250–303
[10] Polf J C, Peterson S, Ciangaru G, Gillin M and Beddar S 2009 *Phys Med Biol* **54** 731–743
[11] Sarrut D, Bardis M, Boussion N, Freud N, Jan S, Ltang J M, Loudos G, Maigne L, Marcatili S, Mauxion T, Papadimitroulas P, Perrot Y, Pietrzyk U, Robert C, Schaart D R, Visvikis D and Buvat I 2014 *Medical Physics* **41**